

In vitro toxicity of Fe_mO_n , $\text{Fe}_m\text{O}_n\text{-SiO}_2$ composite, and $\text{SiO}_2\text{-Fe}_m\text{O}_n$ core-shell magnetic nanoparticles

Yana G Toropova,¹ Alexey S Golovkin,² Anna B Malashicheva,^{3,4} Dmitry V Korolev,^{5,6} Andrey N Gorshkov,⁷ Kamil G Gareev,⁸ Michael V Afonin,⁹ Michael M Galagudza^{10,11}

¹Laboratory of Cardioprotection, Institute of Experimental Medicine, Federal Almazov North-West Medical Research Centre, Saint Petersburg, Russian Federation; ²Gene and Cell Engineering Group, Institute of Molecular Biology and Genetics, Federal Almazov North-West Medical Research Centre, Saint Petersburg, Russian Federation; ³Laboratory of Molecular Cardiology, Institute of Molecular Biology and Genetics, Federal Almazov North-West Medical Research Centre, Saint Petersburg, Russian Federation; ⁴Department of Embryology, Faculty of Biology, Saint Petersburg State University, Saint Petersburg, Russian Federation; ⁵Laboratory of Nanotechnology, Institute of Experimental Medicine, Federal Almazov North-West Medical Research Centre, Saint Petersburg, Russian Federation; ⁶Department of Photonics and Optical Information Technology ITMO University, Saint Petersburg, Russian Federation; ⁷Laboratory of Intracellular Signaling and Transport Research Institute of Influenza, Saint Petersburg, Russian Federation; ⁸Department of Micro and Nanoelectronics, Faculty of Electronics, Saint Petersburg Electrotechnical University LETI, Saint Petersburg, Russian Federation; ⁹Department of Inorganic Chemistry Saint Petersburg State Technological Institute (Technical University), Saint Petersburg, Russian Federation; ¹⁰Institute of Experimental Medicine, Federal Almazov North-West Medical Research Centre, Saint Petersburg, Russian Federation; ¹¹Department of Pathophysiology, First Pavlov State Medical University of Saint Petersburg, Saint Petersburg, Russian Federation

Correspondence: Michael M Galagudza
Institute of Experimental Medicine, Federal Almazov North-West Medical Research Centre, Parkhomenko Str., 15B, Saint Petersburg 194156, Russian Federation
Email galagudza@almazovcentre.ru

Abstract: Over the last decade, magnetic iron oxide nanoparticles (IONPs) have drawn much attention for their potential biomedical applications. However, serious in vitro and in vivo safety concerns continue to exist. In this study, the effects of uncoated, $\text{Fe}_m\text{O}_n\text{-SiO}_2$ composite flake-like, and $\text{SiO}_2\text{-Fe}_m\text{O}_n$ core-shell IONPs on cell viability, function, and morphology were tested 48 h postincubation in human umbilical vein endothelial cell culture. Cell viability and apoptosis/necrosis rate were determined using 3-(4,5-dimethylthiazol-2-yl)-2,5-diphenyltetrazolium bromide assay and annexin V-phycoerythrin kit, respectively. Cell morphology was evaluated using bright-field microscopy and forward and lateral light scattering profiles obtained with flow cytometry analysis. All tested IONP types were used at three different doses, that is, 0.7, 7.0, and 70.0 μg . Dose-dependent changes in cell morphology, viability, and apoptosis rate were shown. At higher doses, all types of IONPs caused formation of binucleated cells suggesting impaired cytokinesis. $\text{Fe}_m\text{O}_n\text{-SiO}_2$ composite flake-like and $\text{SiO}_2\text{-Fe}_m\text{O}_n$ core-shell IONPs were characterized by similar profile of cytotoxicity, whereas bare IONPs were shown to be less toxic. The presence of either silica core or silica nanoflakes in composite IONPs can promote cytotoxic effects.

Keywords: iron oxide nanoparticles, composite nanoparticles, silica coating, silica nanoflakes, cytotoxicity

Introduction

Magnetic iron oxide nanoparticles (IONPs, <150 nm in diameter) are made of magnetite, Fe_3O_4 and/or maghemite, $\gamma\text{-Fe}_2\text{O}_3$. Over the last decade, IONPs have drawn much attention for their potential biomedical applications.^{1,2} In particular, IONPs have been extensively tested experimentally as contrast agents for magnetic resonance imaging (MRI),³ nanoplatforms for multimodal imaging,⁴ targeted drug and gene delivery,^{5,6} stem cell labeling,⁷ hyperthermic tumor therapy,⁸ and also as high-resolution nanosensors.⁹ The advantages of IONPs include high surface area, monodispersity, superparamagnetic properties, and easiness of functionalization offering different strategies of ligand immobilization, which in turn results in tunable release kinetics.¹⁰ Some of IONP-based drugs are already on the market. For example, dextran-coated IONPs (Endorem in Europe or Feridex in USA) are approved by the Food and Drug Administration as contrast agents for MRI imaging of liver tumors.¹¹ NanoTherm™ commercialized by MagForce AG (Berlin, Germany) contains aminosilane-coated 15-nm IONPs which are successfully used for treatment of prostate cancer and glioblastoma after local administration and application of alternating magnetic field resulting in local heating of the tumor tissue up to 45°C.^{12,13} Despite intensive investigation of IONPs for biomedical applications, including first reports on clinical use, serious safety concerns continue to exist. Numerous in vitro and in vivo studies

demonstrated significant toxicity of IONPs with excessive free iron-mediated reactive oxygen species (ROS) formation as a major underlying mechanism resulting in cell necrosis/apoptosis (for review, see Patil et al¹⁴ and Arami et al¹⁵ and references therein). It has been previously shown that the toxicological profile of IONPs depends on such characteristics as diameter, shape, and the presence of coating. In general, more iron ions could be released from higher surface area of smaller IONPs, therefore resulting in greater toxicity. The shape of IONPs seems to be an independent determinant of toxicity because rod-shaped IONPs were shown to be more toxic compared to spherical ones,¹⁶ which might be explained by higher aspect ratio of the former. In the majority of studies, bare IONPs demonstrated greater toxicity in comparison with coated IONPs.¹⁴ However, recent reports have challenged this view; for example, oleate-coated 5–13 nm IONPs possessed higher cyto- and genotoxicity than naked IONPs.¹⁷ Although oleate itself was not found to be cytotoxic, it somehow modified the internalization of nanoparticles and cellular response to IONP accumulation. Silica coating is commonly used to passivate IONPs;^{18,19} however, at present it is not known whether the presence of silica core or silica nanoflakes in the composite IONPs will affect their cytotoxicity.

In this study, we were interested to compare the cytotoxicity of IONPs synthesized by three different methods. The effects of bare, silica-iron oxide composite, and SiO₂-Fe_mO_n core-shell structured IONPs on cell viability, function, and morphology were tested in human umbilical vein endothelial cells (HUVECs). All three tested IONP types were used at three different doses. The results of the study showed dose-dependent increase in IONP cytotoxicity and, importantly, paradoxical increase of toxicity in silica-containing IONPs.

Materials and methods

Synthesis of IONPs

All chemicals were purchased from Sigma-Aldrich (St Louis, MO, USA). Bare IONPs were synthesized by coprecipitation of ferrous and ferric iron ion solutions. Briefly, the mixture of 25% NH₄OH and 1% ammonium acetate was added to FeSO₄ and Fe₂(SO₄)₃ (molar ratio 2:1) in 700 mL of distilled water under intensive stirring at a rate of 4 mL/min until the pH had increased to 8.0. At that moment, black precipitate could be visualized in the solution. The precipitate was separated by centrifugation and washed with distilled water four times. Dry powder of IONPs was prepared by filtration of precipitate and its lyophilization at -48°C for 48 h. Powdered IONPs were added to sterile 0.9% NaCl solution prior to cytotoxicity tests.

Fe_mO_n-SiO₂ composite flake-like IONPs were synthesized by coprecipitation of aqueous solution containing FeCl₃·6H₂O and FeSO₄·7H₂O with ammonia. After magnetic separation, IONPs were resuspended in distilled water followed by addition of tetraethyl orthosilicate (TEOS). The hydrolysis and condensation of TEOS onto IONPs were completed in 7 days, after which the particles were separated with magnetic precipitation, washed five times with distilled water, resuspended in sterile normal saline, and sonicated immediately before use.

SiO₂ core/Fe_mO_n shell IONPs were prepared as described elsewhere.²⁰ In brief, aqueous solution of ammonia was added to isopropanol-dissolved TEOS. The product was dried at room temperature for 7 days and then exposed to 300°C for 30 min. The obtained silica powder was added to the aqueous solution of FeCl₃·6H₂O plus FeSO₄·7H₂O and sonicated. This was followed by the addition of ammonia in distilled water. SiO₂-Fe_mO_n core-shell IONPs were isolated by magnetic precipitation, washed with distilled water, and prepared for cell culture experiments.

Characterization of IONP physicochemical properties

Particle size and morphology of IONPs were assessed by transmission electron microscopy (TEM; JEM-2010, JEOL, Tokyo, Japan). IONPs were dispersed in distilled water and sonicated before TEM study. Atomic force microscopy (NTE-GRA Therna, NT-MDT, Zelenograd, Russian Federation) was used to visualize Fe_mO_n-SiO₂ composite flake-like and SiO₂-Fe_mO_n core-shell IONPs deposited from aqueous solutions on a glass substrate. Dynamic light scattering (DLS) with noninvasive back-scatter technology was used for the determination of hydrodynamic diameters of IONPs (Zetasizer Nano ZS, Malvern Instruments Ltd., Worcestershire, UK). The static magnetic properties of dried IONPs were analyzed at 300 K using vibrating sample magnetometer (Lake Shore 7410, Lake Shore Cryotronics Inc., Westerville, OH, USA). Fourier transform infrared (FTIR) spectra were determined on FTIR spectrometer (NICOLET 6700, Thermo Scientific, Waltham, MA, USA) over a potassium bromide pellet.

Cell culture and cell exposure to IONPs

The study was approved by the ethics committee of the Federal Almazov North-West Medical Research Centre (St Petersburg, Russian Federation). Informed consent was obtained from all patients. In vitro toxicity of IONP preparations was studied on cultured HUVECs. HUVECs were isolated according to standard protocol²¹ and cultured using

endothelial cell culture medium and endothelial cell growth supplement (BD Biosciences, San Jose, CA, USA). The cells were seeded at a density of $5 \times 10^3/\text{cm}^2$ onto gelatinized plates (0.2% of gelatin in phosphate-buffered saline [PBS]). The incubation was performed in a CO_2 incubator at 37°C in humid air containing 5% CO_2 in a 96-well plate for 3–(4, 5-dimethylthiazol-2-yl)-2,5-diphenyltetrazolium bromide (MTT) test and in a 12-well plate for necrosis/apoptosis detection. Each well contained $\sim 100 \times 10^3$ cells in 100 μL of culture medium. HUVECs were treated with 0.7, 7.0, and 70.0 μg of IONPs suspended in 1.0, 10.0, and 100.0 μL of sterile saline, respectively. In all experiments, the cells were incubated with IONPs for 48 h. Pure saline at the same volume was used as control to each IONP concentration. All experiments were performed in triplicate.

Assessment of cell morphology

Morphology of living cells was studied 48 h after cell exposure to IONPs using bright field and phase contrast microscopy at $50\times$ (AxioStar, Carl Zeiss, Germany). The number of binucleated cells was calculated by averaging the value obtained in five random fields of view from each specimen. Both cell size and morphology were also evaluated using forward and lateral light scattering profiles obtained with flow cytometry analysis (Guava EasyCyte 8, Millipore, Billerica, MA, USA). Mathematical processing and imaging of the flow cytometry data were performed by using KaluzaTM v.1.2 (Beckman Coulter, CA, USA) software.

Detection of apoptosis/necrosis

After 48 h of incubation with IONPs, HUVECs were removed from the surface of the plate using trypsin-versene mixture (Lonza Bioscience, Rockland, ME, USA). The cells were stained using annexin V-phycoerythrin (PE; R&D Systems, Minneapolis, MN, USA) according to manufacturer's recommendations and analyzed by flow cytometry. The number of apoptotic and necrotic, annexin V-positive cells were expressed as a percentage of all analyzed cells.

Cell viability measurements

Cell viability was assessed using standard colorimetric MTT assay. At 48 h postincubation, culture medium in each well was replaced with 100 μL MTT (5 mg/mL in PBS solution). After 2 h of incubation at 37°C , culture supernatants were aspirated. Formazan crystals within viable cells were dissolved in 100 μL of dimethyl sulfoxide, whereas precipitated cells were resuspended for 5 min by pipetting. The concentration of reduced MTT in each well was measured at 550 nm using

microplate reader (BioRad Model 680, Bio-Rad Laboratories, Inc., Hercules, CA, USA). Cell viabilities were presented as the percentage of the absorbance of IONP-treated cells to the absorbance of nontreated cells and plotted as IONP concentration. The experiments were repeated three times.

Statistical analysis

All of the data are expressed as the mean \pm standard deviation. The statistical analyses were performed using the SPSS 13.0 software package (SPSS Inc., Chicago, IL, USA). Significant differences between groups were evaluated using analysis of variance. *P*-values ≤ 0.05 were considered significant.

Results

Physicochemical properties of IONPs

Three different methods of IONP synthesis are shown in schematic form in Figure 1. According to TEM imaging, bare IONPs were rod-shaped with mean sizes of 10.5 ± 2.57 nm in diameter and 42.7 ± 6.82 nm in length (Figure 2A), suggesting that the nucleation process was initiated by $\gamma\text{-Fe}_2\text{O}_3$. Using TEM characterization, $\text{Fe}_m\text{O}_n\text{-SiO}_2$ composite flake-like and $\text{SiO}_2\text{-Fe}_m\text{O}_n$ core-shell IONPs demonstrated spherical shape with mean diameter of 98 ± 22 and 101 ± 19 nm, respectively (Figure 2B–E). $\text{Fe}_m\text{O}_n\text{-SiO}_2$ composite IONPs consisted of irregularly ordered nanoflakes of iron oxide and silica (Figure 2B, inset). In TEM images of $\text{SiO}_2\text{-Fe}_m\text{O}_n$ core-shell IONPs, silica core was not visible probably because of the interference of electron-dense iron oxide shell (Figure 2C, inset). Atomic force microscopy images show no visible aggregates of $\text{Fe}_m\text{O}_n\text{-SiO}_2$ composite IONPs (Figure 2D) and aggregation of $\text{SiO}_2\text{-Fe}_m\text{O}_n$ core-shell IONPs (Figure 2E) on a glass substrate. The aggregates of $\text{SiO}_2\text{-Fe}_m\text{O}_n$ core-shell IONPs are presumably forming during their drying because of an increase of concentration. Hydrodynamic diameters did not differ between $\text{Fe}_m\text{O}_n\text{-SiO}_2$ composite flake-like and $\text{SiO}_2\text{-Fe}_m\text{O}_n$ core-shell IONPs and were close to their original size, whereas bare IONPs demonstrated significant aggregation that does not allow estimation of their size using DLS because this method is only applicable for particles $< 10 \mu\text{m}$ (Figure 2F). Mass magnetization curves of IONPs are shown in Figure 2G. The saturation mass magnetization (*M*) of $\text{Fe}_m\text{O}_n\text{-SiO}_2$ composite and $\text{SiO}_2\text{-Fe}_m\text{O}_n$ core-shell IONPs was estimated to be 11.0 emu/g, whereas uncoated IONPs were characterized by $M = 37.2$ emu/g. The lower saturation mass magnetization of SiO_2 -containing IONPs is most likely explained by the presence of nonmagnetic silica inclusions. The lack of hysteresis loop on magnetization curves for all three types of IONPs indicates a superparamagnetic behavior of the nanoparticles.

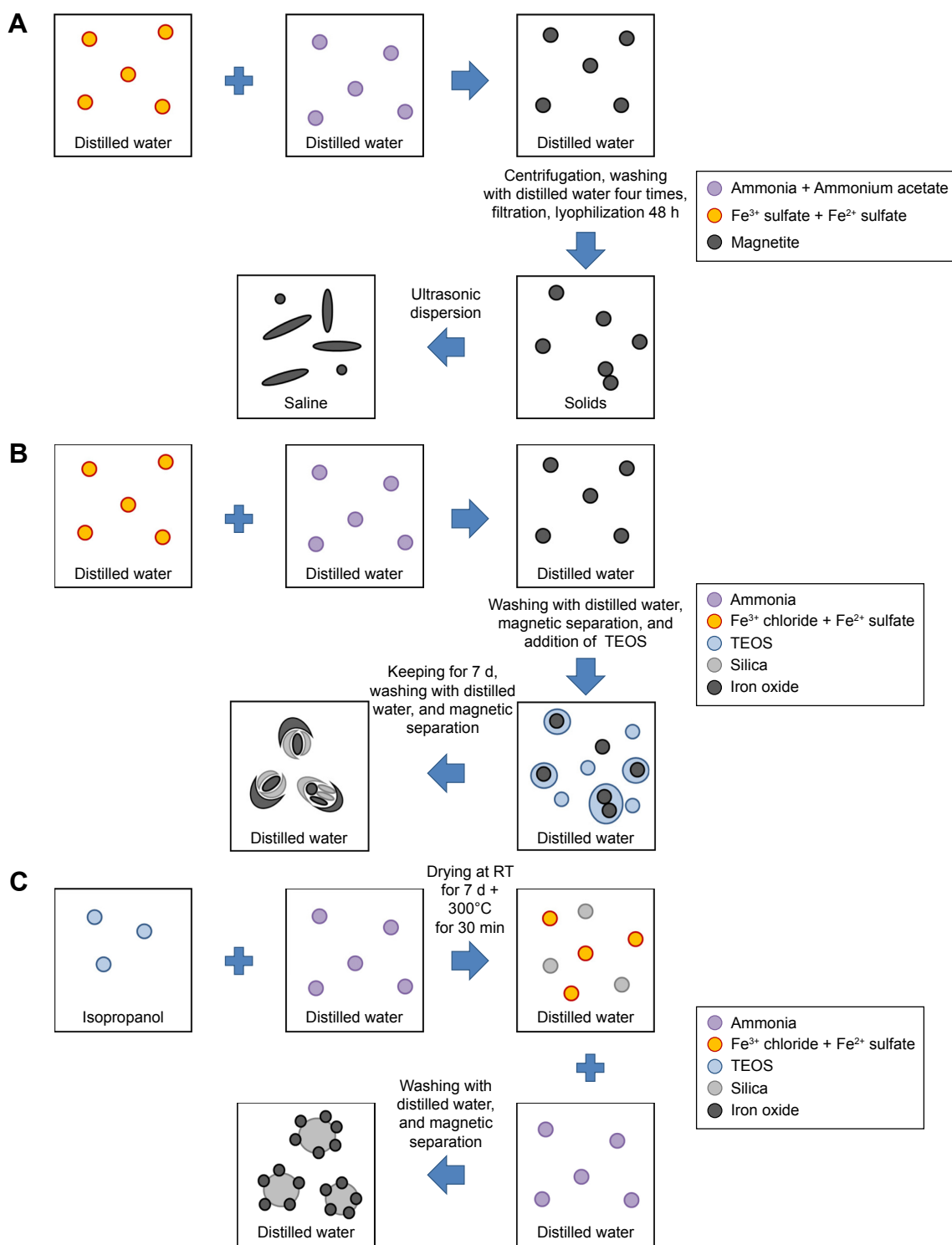


Figure 1 Schematic depiction of IONP synthesis.

Notes: (A) Uncoated IONPs; (B) Fe_mO_n-SiO₂ composite IONPs; (C) Silica-iron oxide core-shell structured IONPs.

Abbreviations: IONPs, magnetic iron oxide nanoparticles; RT, room temperature; TEOS, tetraethyl orthosilicate.

Figure 2H shows the FTIR spectrum of three types of IONPs. All three types of IONPs demonstrated eight typical peaks at 700, 800, 900, 1,100, 1,400, 1,660, 3,100, and 3,400 cm⁻¹, which suggests that iron oxide exists in all IONPs in the same crystalline phase, that is, magnetite and/or maghemite. The

FTIR spectra of SiO₂-containing IONPs exhibited absorbance at 1,100 cm⁻¹, which can be attributed to asymmetric vibration stretching of the Si-O-Si bridges. Bare IONPs were characterized by the peak around 3,100 cm⁻¹ due to O-H stretching mode vibration (Figure 2H).

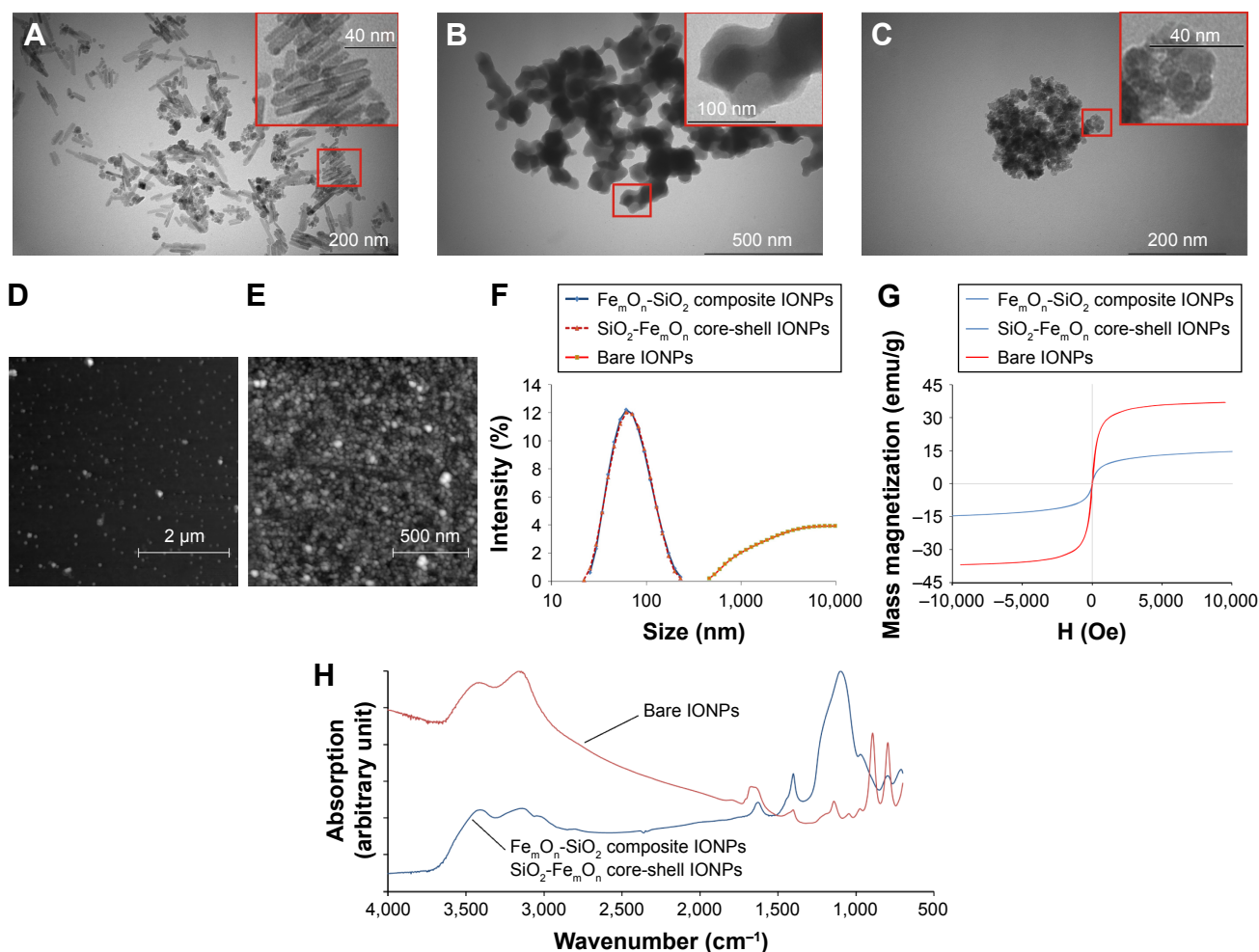


Figure 2 Characteristics of IONPs.

Notes: (A) TEM image of bare IONPs. (B) TEM image of $\text{Fe}_m\text{O}_n\text{-SiO}_2$ composite IONPs. (C) TEM image of $\text{SiO}_2\text{-Fe}_m\text{O}_n$ core-shell IONPs. (D) and (E) Atomic force microscopy image of $\text{Fe}_m\text{O}_n\text{-SiO}_2$ composite and $\text{SiO}_2\text{-Fe}_m\text{O}_n$ core-shell IONPs, respectively. (F) Hydrodynamic diameters of IONPs as measured by dynamic light scattering. (G) Room temperature mass magnetization curves for IONPs. (H) Fourier transform infrared spectra of IONPs.

Abbreviations: IONPs, magnetic iron oxide nanoparticles; TEM, transmission electron microscopy.

IONP-induced changes in cell morphology

No changes in cell morphology were detectable 48 h after vehicle treatment using bright-field microscopy (Figure 3A–C). Incubation of HUVECs with $0.7\ \mu\text{g}$ of three tested IONP types was not associated with significant cell morphology changes (Figure 3D, G, and J). Exposure of HUVECs to bare IONPs, $\text{Fe}_m\text{O}_n\text{-SiO}_2$ composite and $\text{SiO}_2\text{-Fe}_m\text{O}_n$ core-shell IONPs at a dose of $7.0\ \mu\text{g}$ resulted in formation of extracellular IONP aggregates of variable shape and size as well as accumulation of IONPs in the cytoplasm (Figure 3E, H, and K). There were no binucleated cells in controls, while HUVEC exposure to IONPs resulted in their appearance, possibly due to impaired cytokinesis (Table 1). The increase in the number of binucleated cells was generally proportional to the dose of IONPs in a range of $0.7\text{--}7.0\ \mu\text{g}$. All types of IONPs at a dose of $70.0\ \mu\text{g}$ caused significant

cytotoxicity with only occasional cells remaining available for assessment of morphology (Figure 3F, I, and L).

IONP-induced changes in cell size and structure were further investigated using forward and side scattering profiles obtained with flow cytometry analysis (Figure 4). Cell size and structure remained unchanged after incubation with $0.7\ \mu\text{g}$ of all IONPs (Figure 4D, G, and J) when compared with vehicle-treated controls (Figure 4A–C). Administration of $7.0\ \mu\text{g}$ of IONPs resulted in significant changes in cell morphology and granularity without associated changes in cell size (Figure 4E, H, and K). This effect was most pronounced in cells treated with bare IONPs. The application of $\text{Fe}_m\text{O}_n\text{-SiO}_2$ composite and $\text{SiO}_2\text{-Fe}_m\text{O}_n$ core-shell IONPs at a dose of $70.0\ \mu\text{g}$ caused massive cell death as evidenced by nearly complete disappearance of cells from gated area (Figure 4I and L). At the same time, some cells with reduced size and increased granularity were identified within gated

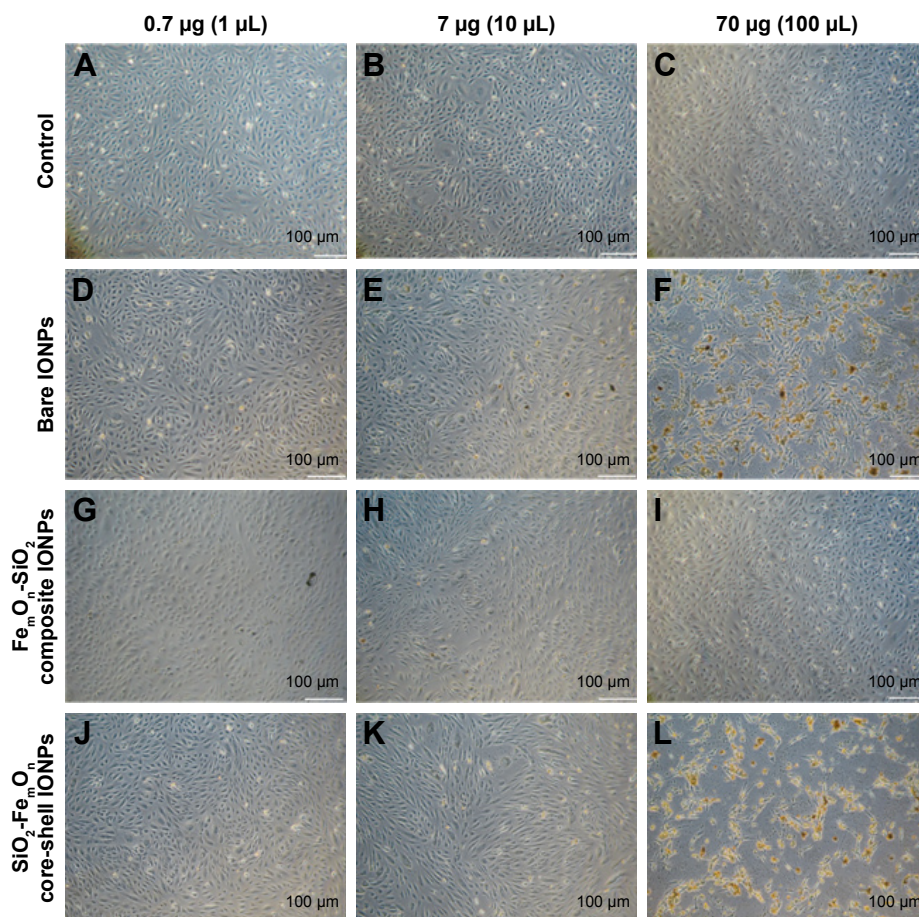


Figure 3 Bright-field microscopy of human umbilical vein endothelial cells with 50 \times magnification 48 h after incubating with IONPs at three different doses; 0.7, 7.0, and 70.0 μ g.

Notes: The images are representative of at least three independent experiments. (A–C) controls; (D–F) bare IONPs; (G–I) $\text{Fe}_m\text{O}_n\text{-SiO}_2$ composite IONPs; and (J–L) $\text{SiO}_2\text{-Fe}_m\text{O}_n$ core-shell IONPs.

Abbreviation: IONPs, magnetic iron oxide nanoparticles.

area 48 h after HUVEC treatment with uncoated IONPs at 70.0 μ g (Figure 4F).

Effects of IONPs on cell death

The percentage of annexin V-positive HUVECs was not different between controls and either bare IONP- or $\text{Fe}_m\text{O}_n\text{-SiO}_2$ composite IONP-treated cells at a dose of 0.7 μ g

Table I The number of binucleated cells per field of view 48 h after incubation of HUVECs with 0.7 and 7.0 μ g of uncoated IONPs, $\text{Fe}_m\text{O}_n\text{-SiO}_2$ composite, and $\text{SiO}_2\text{-Fe}_m\text{O}_n$ core-shell IONPs

	0.7 μ g (1.0 μ L)	7.0 μ g (10.0 μ L)
Bare IONPs	2.8 \pm 1.16*	3.2 \pm 0.74
$\text{Fe}_m\text{O}_n\text{-SiO}_2$ composite IONPs	0.8 \pm 0.49	3.0 \pm 0.63**
$\text{SiO}_2\text{-Fe}_m\text{O}_n$ core-shell IONPs	1.6 \pm 0.75	4.0 \pm 0.62**

Notes: Data are mean \pm standard deviation. * P <0.05 vs $\text{Fe}_m\text{O}_n\text{-SiO}_2$ composite and $\text{SiO}_2\text{-Fe}_m\text{O}_n$ core-shell IONPs; ** P <0.05 vs the dose of 0.7 μ g.

Abbreviations: HUVECs, human umbilical vein endothelial cells; IONPs, magnetic iron oxide nanoparticles.

(Figure 5A). The same dose of $\text{SiO}_2\text{-Fe}_m\text{O}_n$ core-shell IONPs caused significant increase in the number of apoptotic and necrotic cells (24% \pm 2.8% vs 12% \pm 1.8% in controls, P <0.05). While bare IONPs at a dose of 7.0 μ g had no effect on cell death rate, both $\text{Fe}_m\text{O}_n\text{-SiO}_2$ composite and $\text{SiO}_2\text{-Fe}_m\text{O}_n$ core-shell IONPs elicited significant increase in the number of annexin V-positive cells compared with controls (23% \pm 9.5% and 54% \pm 12.8% vs 10% \pm 2.2%, P <0.05 and P <0.01, respectively) and lower dose. HUVEC exposure to 70.0 μ g of IONPs has not changed the number of apoptotic and necrotic cells in comparison with the dose of 7.0 μ g (Figure 5A).

Effects of IONPs on cell viability

All tested types of IONPs did not affect cell viability at a dose of 0.7 μ g (Figure 5B). At a dose of 7.0 μ g, IONPs significantly reduced cell viability in comparison to control. Bare IONPs at a dose of 70.0 μ g had no additional negative

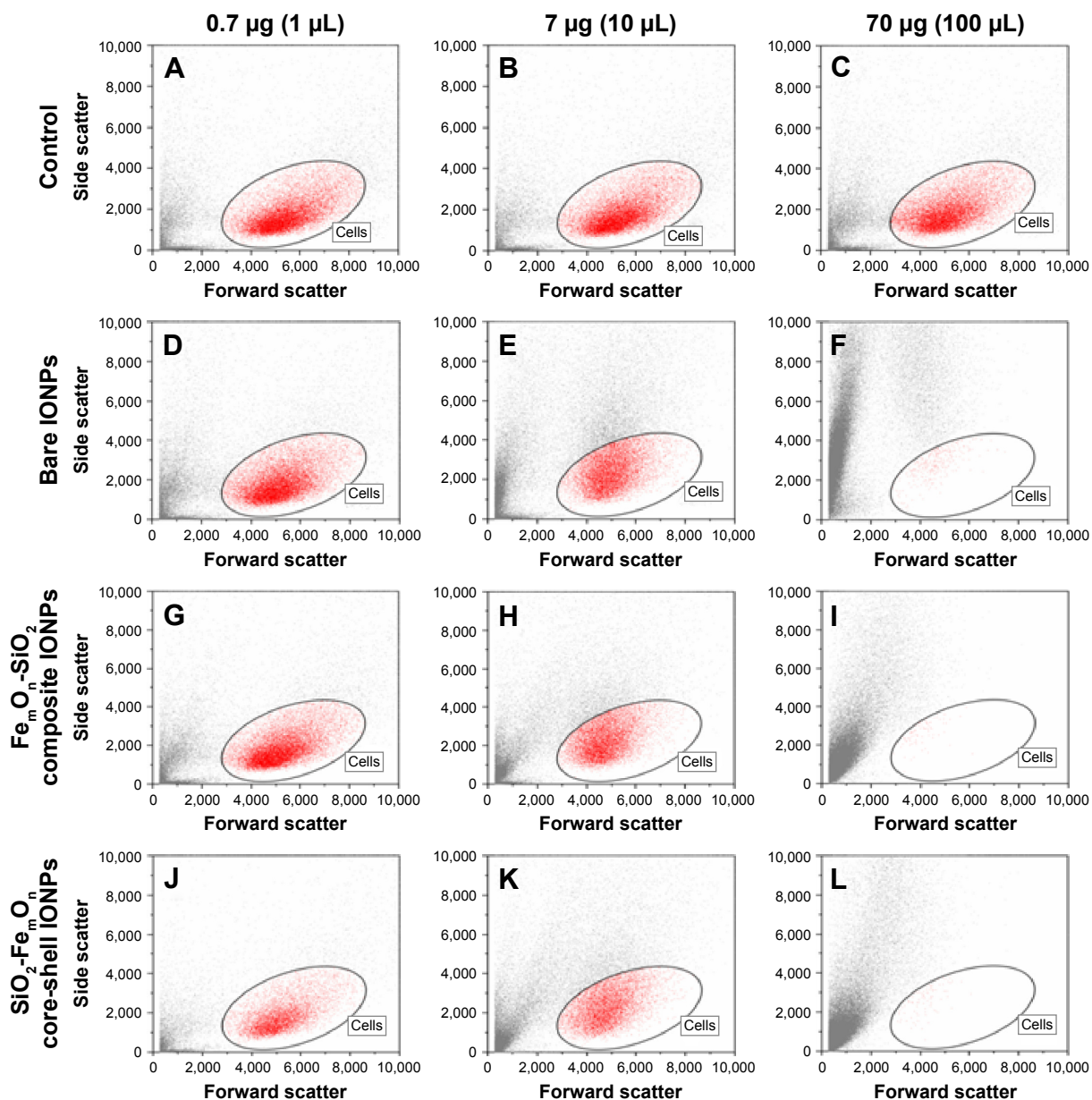


Figure 4 Morphology of human umbilical vein endothelial cells 48 h after incubation with different doses of IONPs according to forward and side scattering profiles obtained with flow cytometry analysis.

Notes: (A–C) Controls; (D–F) Bare IONPs; (G–I) $\text{Fe}_m\text{O}_n\text{-SiO}_2$ composite IONPs; and (J–L) $\text{SiO}_2\text{-Fe}_m\text{O}_n$ core-shell IONPs.

Abbreviation: IONPs, magnetic iron oxide nanoparticles.

impact on cell viability as compared to 7.0 μg , whereas $\text{Fe}_m\text{O}_n\text{-SiO}_2$ composite and $\text{SiO}_2\text{-Fe}_m\text{O}_n$ core-shell IONPs caused additional deterioration in cell viability at the highest dose evaluated (70.0 μg ; Figure 5B).

Discussion

In this study, we thought to compare the effects of three different types of IONPs on cultured HUVECs, which have been chosen as target cells on the basis of the assumption that medical use of IONPs will most likely require intravascular

administration, resulting in extensive contact between IONPs and endothelial cells. The IONP types were bare magnetite nanoparticles, $\text{Fe}_m\text{O}_n\text{-SiO}_2$ composite flake-like IONPs, and $\text{SiO}_2\text{-Fe}_m\text{O}_n$ core-shell structured IONPs. The techniques of bare and $\text{Fe}_m\text{O}_n\text{-SiO}_2$ composite IONP synthesis via Massart²² and Stöber et al²³ methods, respectively, are well characterized and used for investigational and commercial purposes for several decades. In contrast, the two-staged method of Fe_mO_n -coated SiO_2 nanoparticle synthesis was described very recently.²⁰ In this method, presynthesized silica nanoparticles

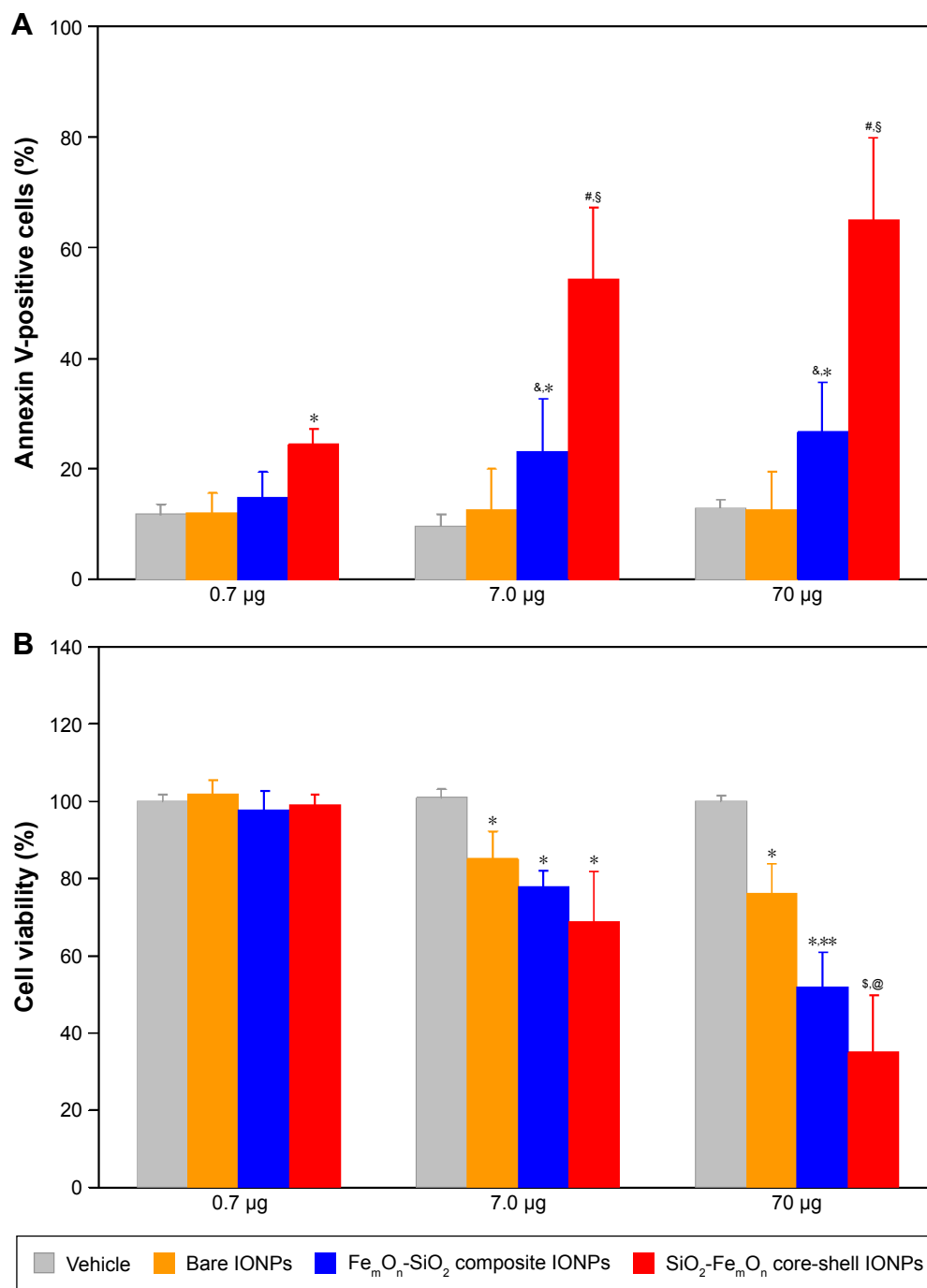


Figure 5 In vitro cytotoxicity of IONPs.

Notes: (A) Percentage of annexin V-positive HUVECs as determined with annexin V-phycoerythrin apoptosis detection kit 48 h after incubation with three different doses of IONPs. * $P < 0.05$ vs vehicle, [&] $P < 0.05$ vs respective value at a dose of 0.7 µg; [#] $P < 0.01$ vs vehicle; [§] $P < 0.05$ vs respective value at a dose of 0.7 µg; (B) 3-(4,5-dimethylthiazol-2-yl)-2,5-diphenyltetrazolium bromide cell viability assay after 48 h of treatment with three different doses of IONPs. * $P < 0.05$ vs vehicle; ^{***} $P < 0.05$ vs respective value at a dose of 7.0 µg; [§] $P < 0.01$ vs vehicle; [@] $P < 0.05$ vs respective value at a dose of 7.0 µg. Data are expressed as means \pm standard deviation.

Abbreviation: IONPs, magnetic iron oxide nanoparticles.

were used as nucleators for the process of iron oxide synthesis by coprecipitation of ferrous and ferric ion solutions. It might be hypothesized that, despite very similar net chemical composition, Fe₃O₄-SiO₂ composite and SiO₂-Fe₃O₄ core-shell IONPs

may demonstrate different behavior when interacting with biological systems, such as cultured cells. As in vitro toxicity of SiO₂-Fe₃O₄ core-shell IONPs has not been studied before, we investigated the effects of HUVEC exposure to bare,

$\text{Fe}_m\text{O}_n\text{-SiO}_2$ composite and $\text{SiO}_2\text{-Fe}_m\text{O}_n$ core-shell IONPs at three different concentrations (0.7, 7.0, and 70.0 μg).

It is generally known that IONP toxicity is mediated through increased production of ROS.¹⁴ Internalization of IONPs in the macrophages or nonphagocytic cells results in the intracellular release of free iron (Fe^{3+}), which stimulates production of highly reactive hydroxyl radicals ($\cdot\text{OH}$) in Fenton reaction.²⁴ If the capacity of endogenous antioxidant systems to quench free radicals is exceeded, excessive ROS may trigger apoptotic cell death via DNA and mitochondrial injury.²⁵ Recent data suggest that the kinetics of ROS formation after cell exposure to IONPs critically depends on physicochemical parameters of IONPs, such as size, shape, and coating. The majority of published studies show that smaller IONPs are more toxic.^{26,27} Indeed, smaller diameters are associated with higher surface area and, consequently, more rapid pattern of Fe^{3+} release with associated oxidative burst. However, this study demonstrated that smaller bare IONPs were less toxic compared to SiO_2 -containing IONPs with larger diameters. In line with this observation, Karlsson et al²⁸ showed that bare 20–30 nm and 5 μm IONPs had similar effect on cell death, mitochondrial injury, and DNA damage in human A549 cells. IONP shape is also considered to be a crucial factor that determines toxicity. For example, incubation of murine macrophages with rod-shaped IONPs resulted in higher prevalence of necrosis in comparison with spherical IONPs.¹⁶ In addition, needle- and plate-shaped nanosized hydroxyapatite particles were demonstrated to be more toxic in BEAS-2B and RAW264.7 cells than sphere- and rod-shaped ones.²⁹ This study provided additional evidence in favor of the idea that spherical shape of IONPs is not necessarily associated with better biocompatibility because rod-shaped bare IONPs were shown to be less toxic in comparison with spherical $\text{Fe}_m\text{O}_n\text{-SiO}_2$ composite IONPs and $\text{SiO}_2\text{-Fe}_m\text{O}_n$ core-shell IONPs.

The presence of coating with specific surface chemistry is another important factor that might affect toxicological profile of IONPs, primarily because of surface passivation and slowing free iron release. The most commonly used IONP coating materials are silica,³⁰ polyethylene glycol,³¹ dextran and its derivatives,³² chitosan,³³ and carbon.³⁴ Very recently, silica-coated IONPs have been tested as contrast agents for biomedical photoacoustic imaging³⁵ and T1 MRI.¹⁸ Most of the available evidence suggests that IONP coating results in reduced toxicity; there are, however, recent studies that have questioned the protective role of the coating. In particular, 3-aminopropyltrimethoxysilane (APTMS)-coated IONPs were shown to have greater negative impact on viability of

fibroblasts and fibrosarcoma cells as compared to bare IONPs and IONPs shielded with TEOS or TEOS/APTMS.²⁷ Another study explored the effects of bare or oleate-covered IONPs on human lymphoblastoid TK6 cells and primary blood cells.¹⁷ Surprisingly, oleate-coated IONPs possessed dose-dependent cyto- and genotoxicity whereas bare IONPs were nontoxic at the equivalent dose. Our results clearly indicate that the presence of either silica core or silica shell substantially increases the toxicity of IONPs. It might be suggested that silica somehow modulates the interaction of IONPs with target cells and/or affects intracellular distribution/degradation of nanoparticles thereby increasing their harmful effect. The difference of the IONPs toxicity can be also due to DLS-documented intensive aggregation of bare IONPs leading to the reduction of the surface area in comparison to $\text{Fe}_m\text{O}_n\text{-SiO}_2$ composite IONPs and $\text{SiO}_2\text{-Fe}_m\text{O}_n$ core-shell IONPs.

Previous studies have shown that high doses of IONPs induce significant changes in morphology of cultured cells, including diminished cell spreading, decreased total area occupied by focal adhesions,³⁶ and altered architecture of microtubule network associated with decreased number of extended microtubules required to induce cell division.³⁷ We suggest that the latter may account for the appearance and dose-dependent increase in the number of binucleated cells observed in this study. Noteworthy, intracellular IONP deposits were predominantly found in binucleated cells, an observation that further supports the connection between IONPs and impaired cytokinesis. Although the mechanism(s) of IONP internalization in the cells were not addressed in this study, strongly increased cell granularity on side-scatter dot plots is indicative of extensive intracellular accumulation of IONPs. Previous work suggests that the most likely ways of IONP internalization are macropinocytosis and clathrin-mediated endocytosis.³⁸ Phagocytic cells can actively engulf magnetic nanowires, as has been recently demonstrated in elegant experiments using selective chemical inhibitors of different internalization pathways.³⁹

Conclusion

In conclusion, uncoated, $\text{Fe}_m\text{O}_n\text{-SiO}_2$ composite, and $\text{SiO}_2\text{-Fe}_m\text{O}_n$ core-shell IONPs induced dose-dependent changes in cell morphology, viability, and apoptosis rate. At higher doses, all types of IONPs caused formation of binucleated cells suggesting impaired cytokinesis. $\text{Fe}_m\text{O}_n\text{-SiO}_2$ composite and $\text{SiO}_2\text{-Fe}_m\text{O}_n$ core-shell IONPs were characterized by a similar profile of cytotoxicity, whereas bare IONPs were less toxic. The presence of either silica core or silica nanoflakes in composite IONPs can promote cytotoxic effects.

Acknowledgments

This study was supported by the Government of Russian Federation (grant 074-U01) and by the Russian Science Foundation (project 14-15-00473). The technique of SiO_2 - Fe_mO_n core-shell IONP and Fe_mO_n - SiO_2 composite IONP synthesis was developed thanks to the support of the Russian Foundation for Basic Research (grant 16-32-60010). Physicochemical parameters of nanoparticles were investigated using equipment at the Resource Center of St Petersburg State University “Innovative technologies of composite nanomaterials”.

Disclosure

The authors report no conflicts of interest in this work.

References

- Reddy LH, Arias JL, Nicolas J, Couvreur P. Magnetic nanoparticles: design and characterization, toxicity and biocompatibility, pharmaceutical and biomedical applications. *Chem Rev.* 2012;112(11):5818–5878.
- Liu G, Gao J, Ai H, Chen X. Applications and potential toxicity of magnetic iron oxide nanoparticles. *Small.* 2013;9(9–10):1533–1545.
- Jin R, Lin B, Li D, Ai H. Superparamagnetic iron oxide nanoparticles for MR imaging and therapy: design considerations and clinical applications. *Curr Opin Pharmacol.* 2014;18:18–27.
- Xie J, Chen K, Huang J, et al. PET/NIRF/MRI triple functional iron oxide nanoparticles. *Biomaterials.* 2010;31(11):3016–3022.
- Mou X, Ali Z, Li S, He N. Applications of magnetic nanoparticles in targeted drug delivery system. *J Nanosci Nanotechnol.* 2015;15(1):54–62.
- Laurent S, Saei AA, Behzadi S, Panahifar A, Mahmoudi M. Superparamagnetic iron oxide nanoparticles for delivery of therapeutic agents: opportunities and challenges. *Expert Opin Drug Deliv.* 2014;11(9):1449–1470.
- Spira D, Bantleon R, Wolburg H, et al. Labeling human melanoma cells with SPIO: in vitro observations. *Mol Imaging.* 2016;15. pii: 1536012115624915.
- Lee JH, Jang JT, Choi JS, et al. Exchange-coupled magnetic nanoparticles for efficient heat induction. *Nat Nanotechnol.* 2011;6(7):418–422.
- Xie J, Zhang F, Aronova M, et al. Manipulating the power of an additional phase: a flower-like $\text{Au-Fe}_3\text{O}_4$ optical nanosensor for imaging protease expressions in vivo. *ACS Nano.* 2011;5(4):3043–3051.
- Gupta AK, Gupta M. Synthesis and surface engineering of iron oxide nanoparticles for biomedical applications. *Biomaterials.* 2005;26(18):3995–4021.
- Li YW, Chen ZG, Wang JC, Zhang ZM. Superparamagnetic iron oxide-enhanced magnetic resonance imaging for focal hepatic lesions: systematic review and meta-analysis. *World J Gastroenterol.* 2015;21(14):4334–4344.
- Johannsen M, Gneveckow U, Thiesen B, et al. Thermotherapy of prostate cancer using magnetic nanoparticles: feasibility, imaging, and three-dimensional temperature distribution. *Eur Urol.* 2007;52(6):1653–1661.
- Maier-Hauff K, Ulrich F, Nestler D, et al. Efficacy and safety of intratumoral thermotherapy using magnetic iron-oxide nanoparticles combined with external beam radiotherapy on patients with recurrent glioblastoma multiforme. *J Neurooncol.* 2011;103(2):317–324.
- Patil US, Adireddy S, Jaiswal A, Mandava S, Lee BR, Chrisey DB. In vitro/in vivo toxicity evaluation and quantification of iron oxide nanoparticles. *Int J Mol Sci.* 2015;16(10):24417–24450.
- Arami H, Khandhar A, Liggitt D, Krishnan KM. In vivo delivery, pharmacokinetics, biodistribution and toxicity of iron oxide nanoparticles. *Chem Soc Rev.* 2015;44(23):8576–8607.
- Lee JH, Ju JE, Kim BI, et al. Rod-shaped iron oxide nanoparticles are more toxic than sphere-shaped nanoparticles to murine macrophage cells. *Environ Toxicol Chem.* 2014;33(12):2759–2766.
- Magdolenova Z, Drlickova M, Henjum K, et al. Coating-dependent induction of cytotoxicity and genotoxicity of iron oxide nanoparticles. *Nanotoxicology.* 2015;9(Suppl 1):44–56.
- Iqbal MZ, Ma X, Chen T, et al. Silica-coated super-paramagnetic iron oxide nanoparticles (SPIONs): a new type contrast agent of T1 magnetic resonance imaging (MRI). *J Materials Chem B.* 2015;3(26):5172–5181.
- Guo X, Mao F, Wang W, Yang Y, Bai Z. Sulfhydryl-modified Fe_3O_4 @ SiO_2 core/shell nanocomposite: synthesis and toxicity assessment in vitro. *ACS Appl Mater Interfaces.* 2015;7(27):14983–14991.
- Bogachev YV, Chernenco JUS, Gareev KG, et al. The study of aggregation processes in colloidal solutions of magnetite–silica nanoparticles by NMR relaxometry, AFM, and UV–vis-spectroscopy. *Appl Magn Reson.* 2014;45(3):329–337.
- Baudin B, Bruneel A, Bosselut N, Vaubourdoles M. A protocol for isolation and culture of human umbilical vein endothelial cells. *Nat Protoc.* 2007;2(3):481–485.
- Massart R. Preparation of aqueous magnetic liquids in alkaline and acidic media. *IEEE T Magn.* 1981;17(2):1247–1248.
- Stöber W, Fink A, Bohn E. Controlled growth of monodisperse silica spheres in the micron size range. *J Colloid Interf Sci.* 1968;26(1):62–69.
- Voinov MA, Pagan JOS, Morrison E, Smirnova TI, Smirnov AI. Surface-mediated production of hydroxyl radicals as a mechanism of iron oxide nanoparticle biotoxicity. *J Am Chem Soc.* 2011;133(1):35–41.
- Circu ML, Aw TY. Reactive oxygen species, cellular redox systems, and apoptosis. *Free Radic Biol Med.* 2010;48(6):749–762.
- Ying E, Hwang HM. In vitro evaluation of the cytotoxicity of iron oxide nanoparticles with different coatings and different sizes in A3 human T lymphocytes. *Sci Total Environ.* 2010;408(20):4475–4481.
- Yang L, Kuang H, Zhang W, et al. Size dependent biodistribution and toxicokinetics of iron oxide magnetic nanoparticles in mice. *Nanoscale.* 2015;7(2):625–636.
- Karlsson HL, Gustafsson J, Cronholm P, Möller L. Size-dependent toxicity of metal oxide particles – a comparison between nano- and micrometer size. *Toxicol Lett.* 2009;188(2):112–118.
- Zhao X, Ng S, Heng BC, et al. Cytotoxicity of hydroxyapatite nanoparticles is shape and cell dependent. *Arch Toxicol.* 2013;87(6):1037–1052.
- Yang W, Lee J, Hong S, Lee J, Lee J, Han DW. Difference between toxicities of iron oxide magnetic nanoparticles with various surface-functional groups against human normal fibroblasts and fibrosarcoma cells. *Materials.* 2013;6(10):4689–4706.
- Al Faraj A. Preferential magnetic nanoparticle uptake by bone marrow derived macrophages sub-populations: effect of surface coating on polarization, toxicity, and in vivo MRI detection. *J Nanopart Res.* 2013;15(7):1–13.
- Easo SL, Mohanan PV. Dextran stabilized iron oxide nanoparticles: synthesis, characterization and in vitro studies. *Carbohydr Polym.* 2013;92(1):726–732.
- Shi SF, Jia JF, Guo XK, et al. Biocompatibility of chitosan-coated iron oxide nanoparticles with osteoblast cells. *Int J Nanomedicine.* 2012;7:5593–5602.
- Grudzinski IP, Bystrzejewski M, Cywinska MA, et al. Cytotoxicity evaluation of carbon-encapsulated iron nanoparticles in melanoma cells and dermal fibroblasts. *J Nanopart Res.* 2013;15:1835.
- Alwi R, Telenkov S, Mandelis A, et al. Silica-coated super paramagnetic iron oxide nanoparticles (SPION) as biocompatible contrast agent in biomedical photoacoustics. *Biomed Opt Express.* 2012;3(10):2500–2509.

36. Soenen SJ, Himmelreich U, Nuytten N, De Cuyper M. Cytotoxic effects of iron oxide nanoparticles and implications for safety in cell labelling. *Biomaterials*. 2011;32(1):195–205.
37. Soenen SJ, Nuytten N, De Meyer SF, De Smedt SC, De Cuyper M. High intracellular iron oxide nanoparticle concentrations affect cellular cytoskeleton and focal adhesion kinase-mediated signaling. *Small*. 2010;6(7):832–842.
38. Calero M, Chiappi M, Lazaro-Carrillo A, et al. Characterization of interaction of magnetic nanoparticles with breast cancer cells. *J Nanobiotechnology*. 2015;13:16.
39. Perez JE, Contreras MF, Vilanova E, et al. Cytotoxicity and intracellular dissolution of nickel nanowires. *Nanotoxicology*. 2016;10(7):871–880.

International Journal of Nanomedicine

Publish your work in this journal

The International Journal of Nanomedicine is an international, peer-reviewed journal focusing on the application of nanotechnology in diagnostics, therapeutics, and drug delivery systems throughout the biomedical field. This journal is indexed on PubMed Central, MedLine, CAS, SciSearch®, Current Contents®/Clinical Medicine,

Submit your manuscript here: <http://www.dovepress.com/international-journal-of-nanomedicine-journal>

Journal Citation Reports/Science Edition, EMBase, Scopus and the Elsevier Bibliographic databases. The manuscript management system is completely online and includes a very quick and fair peer-review system, which is all easy to use. Visit <http://www.dovepress.com/testimonials.php> to read real quotes from published authors.

Dovepress